Physics of Fluids

RESEARCH ARTICLE | JANUARY 30 2024

Shock tube experiments on the three-layer Richtmyer–Meshkov instability

Special Collection: Shock Waves

M. Schalles; C. Louie; K. Peabody; J. Sadler; Y. Zhou; J. Jacobs

Physics of Fluids 36, 014126 (2024)
https://doi.org/10.1063/5.0179296

Physics of Fluids ARTICLE pubs.aip.org/aip/pof

Shock tube experiments on the three-layer Richtmyer–Meshkov instability

Cite as: Phys. Fluids 36, 014126 (2024); doi: 10.1063/5.0179296
Submitted: 1 October 2023 · Accepted: 5 January 2024 ·
Published Online: 30 January 2024

View Online Export Citation CrossMark

M. Schalles,[1] C. Louie,[1] K. Peabody,[1] J. Sadler,[2] Y. Zhou,[2] and J. Jacobs[1,a)]

AFFILIATIONS

[1]Department of Aerospace and Mechanical Engineering, University of Arizona, Tucson, Arizona 85721, USA
[2]Lawrence Livermore National Laboratory, 7000 East Avenue, Livermore, California 94550, USA

Note: This paper is part of the special topic, Shock Waves.
[a)]**Author to whom correspondence should be addressed:** jwjacobs@arizona.edu

ABSTRACT

A vertical shock tube is used for experiments on the three-layer Richtmyer–Meshkov instability. Two closely spaced membrane-less interfaces are formed by the flow of two different sects of three gases: one with air above CO_2 above SF_6 and the other with helium above air above SF_6. The lightest of the three gases enters the shock tube at the top of the driven section and flows downward. Conversely, the heaviest gas enters at the bottom of the shock tube and flows upward while the intermediate density gas enters at the middle through porous plates. All three gases are allowed to escape through holes at the layer location, leaving an approximately 30-mm layer of intermediate-density gas suspended between the lightest gas from above and the heaviest gas from below. A single-mode, two-dimensional initial perturbation is then imposed on the lower interface by oscillating the shock tube in the horizontal direction. The flow is visualized by seeding the intermediate gas with particles and illuminating it with a pulsed laser. Image sequences are then captured using high-speed video cameras. Perturbation amplitude measurements are made from the three-layer system and compared with measurements from 2, two-layer systems. It is observed that the presence of the upper, initially flat interface produces a decrease in growth of instability amplitude in the nonlinear phase over an equivalent single-interface configuration.

I. INTRODUCTION

The Richtmyer–Meshkov instability (RMI) occurs when a perturbed interface between two gases having different densities is impulsively accelerated, typically by a shock wave. The impulsive acceleration causes an initial perturbation to grow and eventually become turbulent. RMI is closely related to the Rayleigh–Taylor instability, which exhibits similar behavior but which is produced by a constant acceleration such as by gravity. The RMI derives its name from the analytical and numerical work of Richtmyer,[1] which was later confirmed in shock tube experiments by Meshkov.[2] RMI is of fundamental importance to a number of applications. For example, it has been attributed as a source of mixing in supernovae[3] and in supersonic combustion.[4] In addition, it has been identified as a major obstacle to achieving positive-net-yield in inertial confinement fusion (ICF)[5] experiments.

There has been a significant amount of work carried out in the study of RMI from theoretical, computational, and experimental perspectives (see recent reviews[6–9] and Refs. 10–15 for recent experimental results). The large majority of previous work has been focused solely on the instability of a single interface separating two different gases. However, it is important to recognize that applications such as ICF involve configurations having multiple, closely spaced interfaces. Multi-interface RMI has received some attention in theoretical, computational, and experimental studies. Mikaelian[16–19] has published extensively on the RMI of multiple-interface configurations in both Cartesian and cylindrical geometries. Computationally, there has been recent work on the numerical simulations of the two-interface RMI.[20] On the experimental side, there have been a number of studies performed at the University of Science and Technology of China, focusing on several different two-interface configurations.[21–26] However, these experiments utilize a soap film to separate the different gases and, therefore, cannot accurately duplicate the vortical structures known to dominate the late-time, nonlinear evolution. It is, therefore, the focus of this study to expand upon previous work by exploring experimentally the RMI of a system consisting of two membrane-less interfaces separating three gases. Specifically, the presence of an unperturbed interface near an evolving RM unstable one is examined for its interactive effect on the growth of the instability.

II. EXPERIMENTAL SETUP

Single-interface, membrane-less Richtmyer–Meshkov instability experiments have been previously carried out in a vertical shock tube at the University of Arizona employing a wide variety of initial perturbation, including both two-dimensional[27–30] and three-dimensional[31] single-mode perturbations, as well as multi-mode semi-random perturbations.[32,33] The present study utilizes the apparatus and experimental techniques of these previous investigations modified to allow the generation of two interfaces separating three gases.

A 5-m long vertical shock tube (shown in Fig. 1) with a 3.7-m long, 10.2-cm diameter circular driver, and a 5.25-m long, 8.9 $\times$ 8.9 cm^2 square driven section, including a 1.1-m long test section is used for this study. The distance between the layer location and the shock tube end wall is 1.05 m. The lightest gas (either helium or air) enters the tube at the top of the driven section immediately below the diaphragm, and the heaviest gas (sulfur hexafluoride) enters at the bottom of the test section, while the intermediate gas (either air or CO_2) enters through two plenums fitted with porous metal plates positioned at opposite sides of the test section. The gases exit the shock tube through two sets of holes in the test section located at the top and bottom of the porous plates, leaving behind a flat layer of intermediate gas of thickness, $h \approx 30$ mm suspended between the light gas from above and the heavy gas from below, separated by two diffuse interfaces. This gas configuration yields two Atwood numbers: $A_{\text{upper}} = \frac{\rho_2-\rho_1}{\rho_2+\rho_1} = 0.21$ for air/CO_2 or 0.76 for He/air and $A_{\text{lower}} = \frac{\rho_3-\rho_2}{\rho_3+\rho_2} = 0.54$ for CO_2/SF_6 or 0.67 for air/SF_6.

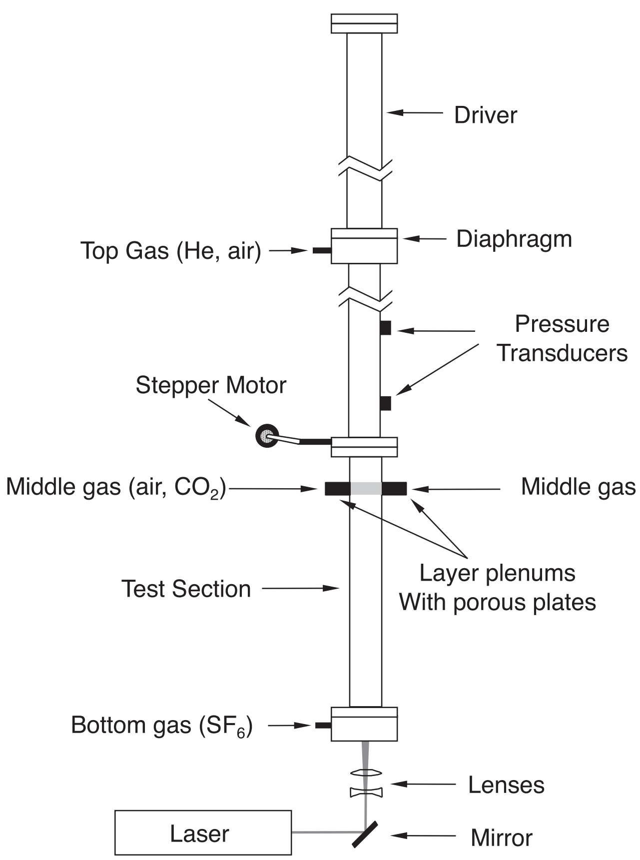

FIG. 1. Drawing of the experimental apparatus.

In addition to the two-interface experiments with the two combinations of gases described earlier, additional single-interface experiments using the two gas combinations: air/SF_6 and CO_2/SF_6 were also carried out for comparison with the two-interface experiments. In these cases, the gas supply to the middle layer was turned off and one set of exit holes was blocked, mimicking earlier experiments carried out at the UA on single-interface RMI.

As has been done in previous studies,[27–30] a two-dimensional, single-mode initial perturbation is generated by periodically oscillating the square shock tube, laterally using a stepper motor and crank mechanism, to produce a two-dimensional standing wave on the lower interface, while no significant perturbation is generated on the upper surface. In the experiments presented here, the perturbation is that of 2.5 waves spanning the test section, yielding a wavenumber of 1.76 cm^{-1}. A $M = 1.177$ shock wave for the air/CO_2/SF_6 experiments and $M = 1.074$ shock wave for the He/air/SF_6 experiments are generated by puncturing a polypropylene diaphragm and travel down the tube where it impacts the interfaces to produce the instability. The firing of the shock tube is synchronized with the motion of the stepper motor to achieve repeatable initial perturbations. Experimental parameters for the experiments presented here are listed in Table I. Here, M is the incident shock Mach number, k is the perturbation wavenumber, a_{0-} is the mean perturbation amplitude measured immediately prior to shock arrival, a_{0+} is the mean perturbation amplitude measured immediately after shock arrival, $SD(a_{0-})$ is the standard deviation of the a_{0-} measurements, A_{lower} is the Atwood number of the lower interface, A_{upper} is the Atwood number of the upper interface, h is the measured initial layer thickness, and V is the measured interface velocity following passage of the shock wave.

The flow is visualized by using planar laser Mie scattering images. As described earlier, the middle layer gas is seeded with 2 μm diameter propylene glycol droplets using the particle generator used by Sewell *et al.*[33] The particles are then illuminated by the second harmonic of a pulsed Nd:YLF laser operated at 6 kHz and positioned at the lower end of the shock tube. The laser's output is passed through spherical and cylindrical lenses and reflected upward through a window in the shock tube end wall, producing a light sheet normal to the camera view that illuminates a thin cross section of the gases. The resulting Mie-scattered images are captured using either four high-speed video cameras in a stacked array or a single higher resolution high-speed camera.

TABLE I. Parameter values for the experiments.

	Air/CO_2/SF_6	CO_2/SF_6	He/air/SF_6	Air/SF_6
M	1.117	1.205	1.074	1.117
k (mm^{-1})	0.177	0.177	0.177	0.177
a_{0-} (mm)	1.64	1.46	2.71	1.62
a_{0+} (mm)	1.03	0.94	2.64	1.26
$SD(a_{0-})$ (mm)	0.22	0.06	0.29	0.19
A_{lower}	0.54	0.54	0.67	0.67
A_{upper}	0.21	NA	0.76	NA
h (mm)	27	NA	29.5	NA
V (m/s)	63	67	46	65

In both cases, the cameras are positioned to cover the full interface evolution, including re-shock.

A total of 20 experiments, 5 of each from the four gas combinations: air/CO_2/SF_6, CO_2/SF_6, He/air/SF_6, and air/SF_6, are presented here.

III. RESULTS AND DISCUSSION

Figure 2 shows a sequence of Mie scattering images taken from a typical air/CO_2/SF_6 experiment. Here, the middle gas (CO_2) has been seeded, making it visible, while the other two unseeded gases are invisible. In this sequence, one can observe the initial perturbation on the lower interface prior to shock interaction, followed by the development of the instability resulting from interaction by the incident shock wave. This is eventually followed by re-shock resulting from the shock wave after having reflected from the shock tube end wall, interacting with the layer a second time. Early in the development, the interface retains a roughly sinusoidal shape. Later on, however, nonlinear effects appear with the formation of vortices, resulting in the mushroom structures observed beginning at approximately $t = 4$ ms. Also, early in the development of the instability, the perturbation on the lower interface grows without influencing the upper interface. However, as the growing spike tips approach the upper, initially unperturbed, interface, the developing mushroom structures begin to interact with the upper interface, eventually deforming it. Following re-shock, the symmetry of the instability is destroyed with the production of increased vorticity resulting from the reflected shock wave interacting with the highly distorted interfaces, resulting in the development of turbulence.

Figure 3 is a similar sequence but shows the evolution of an He/air/SF_6 experiment. In this case, air forms the seeded middle layer. Relative to the air/CO_2/SF_6, the lower interface spikes approach the upper interface more quickly and break down more significantly before the reflected shock arrives at approximately $t = 11$ ms. One noticeable difference between this experiment and the air/CO_2/SF_6 of Fig. 2 is that the quality of the evolving interfaces changes drastically at $t = 7$ ms with the destruction of the mushroom structures and an apparent penetration of the heaviest gas (SF_6) into the lightest gas (helium). This is, in addition, accompanied by an apparent rapid transition to turbulence.

Figures 4 and 5 show two single-interface experiments designed to illustrate the evolution of the instabilities depicted in Figs. 2 and 3 but in the absence of the upper unperturbed interface. A sinusoidal initial perturbation comparable to that on the lower interface of three-layer experiments is formed in this case on the sole interface. The CO_2/SF_6 experiment shows a similar development of mushroom structures as vorticity coalesces at the spikes at roughly $t = 5$ ms. The appearance of these similarly shaped structures demonstrates that in two-layer cases, the instability develops largely the same as in the three-layer cases before interaction between the interfaces would begin.

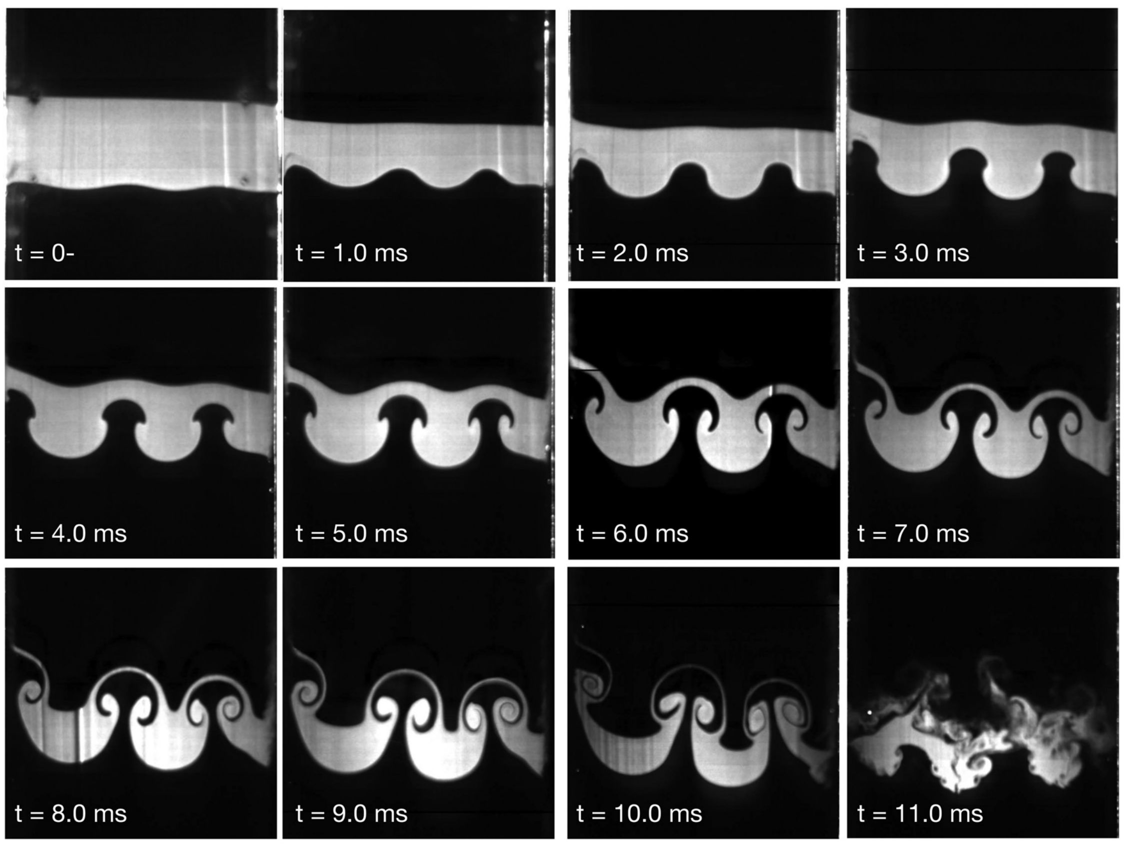

FIG. 2. Image sequence of an air/CO_2/SF_6 experiment.

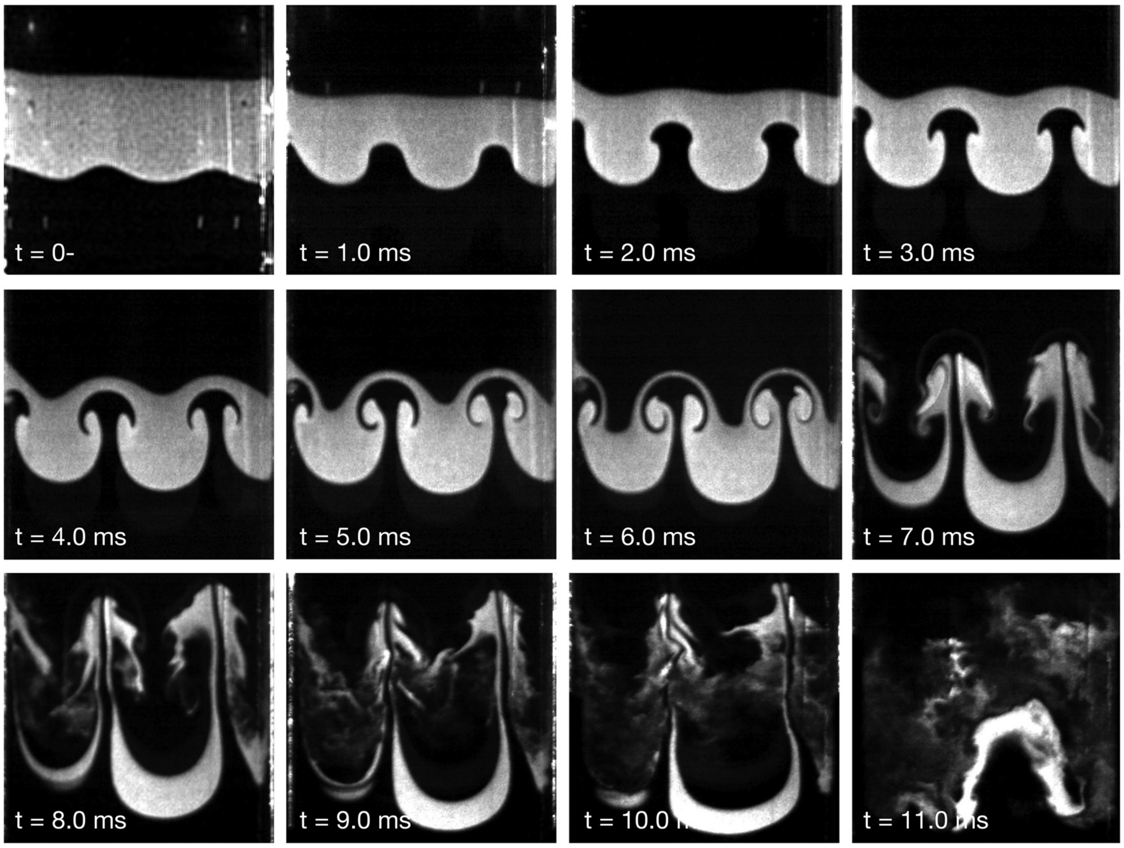

FIG. 3. Image sequence of an He/air/SF_6 experiment.

Figure 5 likewise shows an air/SF_6 single-interface experiment corresponding to the He/air/SF_6 experiments. Like He/air/SF_6, vortices develop more quickly and more intensely, with the presence of secondary instability, relative to the CO_2/SF_6 case, due to its larger Atwood number.

The perturbation amplitude, defined as one-half the height difference between the crest and the trough, was measured by determining the locations of the leftmost fully formed peak and rightmost fully formed trough in each frame as shown in Fig. 6. These values were determined by finding the maximum vertical gradient of image brightness across a frame and taking the highest point at which this maximum occurs as the crest height and the lowest point at which it occurs as the trough height. Figure 7 shows the growth in amplitude of the five air/CO_2/SF_6 experiments. Note that the curves differ primarily due to differences in initial perturbation amplitudes. The shape of the individual growth curves is very similar to that of single-interface, single-mode RMI, such as observed by Jacobs and Krivets.[29] For comparison, a plot of five "control" single-interface CO_2/SF_6 experiments is also shown, exhibiting the same type of behavior.

Figure 8 shows equivalent two-interface, He/air/SF_6, and control, single-interface, air/SF_6 experiments. The instability amplitudes initially grow linearly with time as predicted by linear stability theory. However, when nonlinearity becomes important, the growth rate decreases with increasing amplitude.

An important question that we would like to address here is: How does the presence of the upper interface affect the growth of the instability on the lower interface? To answer this, it becomes important to compare the growth of the two-interface instability with that of an equivalent single-interface control experiment. Since we are considering the RMI of the growth of only the lower interface in a two-interface system, it is logical to compare growth with a single-interface experiment having the same two gases as the middle and bottom gases. However, it is also important to recognize that in this case, the direct comparison of amplitude measurements is not appropriate since the impulse velocity, V, produced by a shock wave of the same strength will differ between an air/CO_2/SF_6 configuration and a CO_2/SF_6 or between an He/air/SF_6 and an air/SF_6 one. In addition, while we attempt to keep the initial perturbation amplitudes of the three cases the same, they differ owing to the different gas combinations along with random run-to-run variation. These two factors make comparing single- and two-interface experiments in dimensional form virtually impossible. However, because it is expected that the instability amplitudes in all four cases should initially grow as described by linear stability theory, i.e.,

$$a = a_0 + ka_0AVt = a_0 + \dot{a}_0t,$$

where a is the amplitude, k is the wavenumber, a_0 is the initial amplitude, A is the Atwood number, V is the impulse to the interface imparted by the shock wave, $\dot{a}_0$ is the initial growth rate, and t is time,

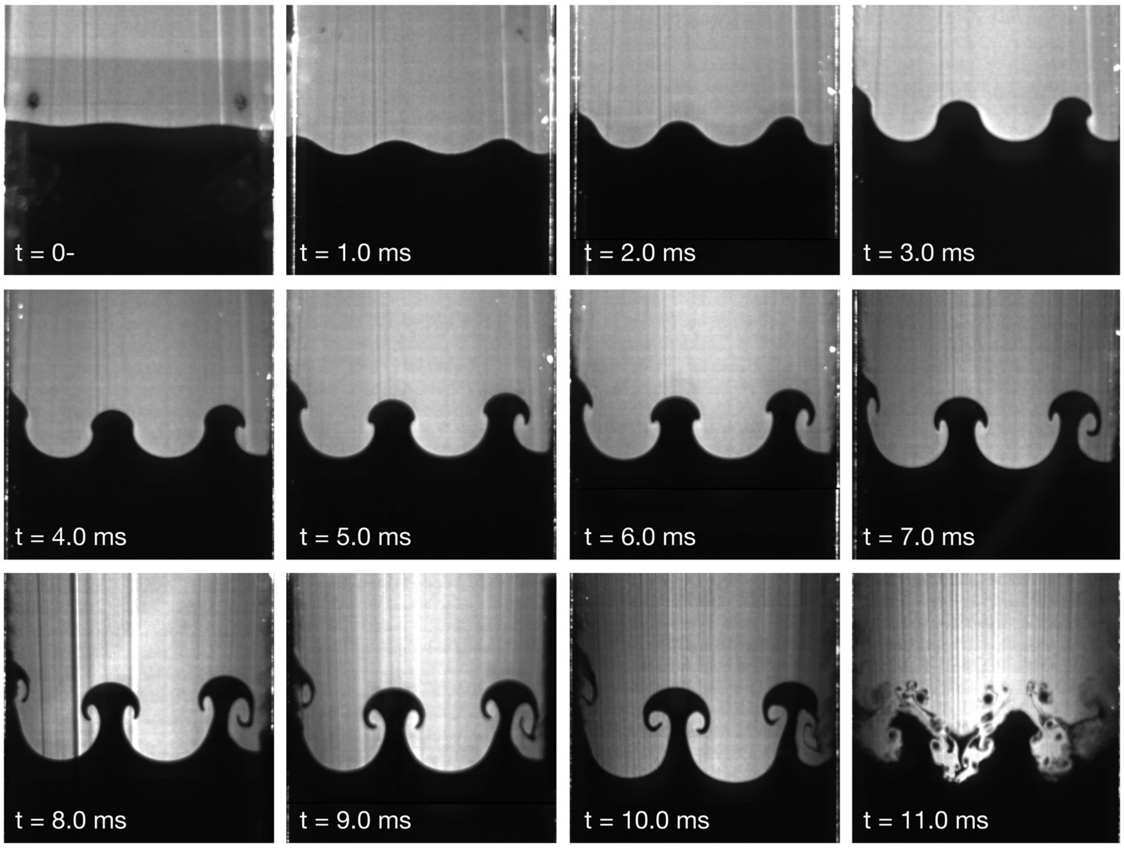

FIG. 4. Image sequence of a CO_2/SF_6 experiment.

an appropriate comparison may be made using the dimensionless coordinates defined by Jacobs and Krivets,[29] i.e., $k(a - a_0)$ vs $k\dot{a}_0 t$, which effectively collapses the linear growth of experiments having different gas combinations, initial amplitudes, and Mach numbers. This allows for the comparison of differences in the nonlinear growth behavior, which is where we expect to observe the effects of the upper interface on the developing instability of the lower interface. It should be noted that we do not use $\dot{a}_0 = ka_0AV$ to evaluate the initial growth rate since, for it to be accurate, it requires modification to account for the effect of initial interfacial diffusion thickness as has been previously shown.[28,29] Instead we use the measured initial growth rate obtained from linear curve-fits of the first five post-shock amplitude measurements for each experiment. This ensures a good collapse of the data in the early linear stage, allowing for comparison of differences at later times where the effects of interaction with the upper interface are expected to be revealed.

Figure 9 is a plot of the amplitude measurements in Fig. 7 but using the dimensionless variables defined by Jacobs and Krivets, i.e., $k(a - a_0)$ vs $k\dot{a}_0 t$, where in this case $\dot{a}_0$ is found from a curve fit of amplitude measurements for each experiment. In comparing the air/CO_2/SF_6 and CO_2/SF_6 experiments in Fig. 9, it is apparent that the two-interface amplitudes lie slightly below the single-interface amplitudes, indicating that the presence of the upper unperturbed interface may have a slight effect on reducing the growth rate in the nonlinear stage. However, this difference is small and comparable in size to the run-to-run variation.

Figure 10 shows the amplitude measurements of Fig. 8 comparing the He/air/SF_6 experiments with the air/SF_6 experiments plotted in the dimensionless variables of Jacobs and Krivets.[29] In this case, again, the dimensionless variables do well in collapsing the curves at early times, allowing the nonlinear growth behavior to be highlighted. However, in comparing the air/SF_6 growth curves with those of He/air/SF_6, a larger difference can be observed with the two-interface experiments on average lying well below the single-interface control experiments. Thus, it appears that the presence of the He/air interface above the air/SF_6 interface reduces the growth of the instability in the nonlinear regime. Also shown in Fig. 10 is a curve representing the model of Sadot *et al.*,[34]

$$\frac{\dot{a}_{b/s}}{\dot{a}_0} = \frac{1 + k\dot{a}_0 t}{1 + (1 \pm A)k\dot{a}_0 t + E(k\dot{a}_0 t)^2},$$

$$E = \begin{cases} \dfrac{3}{2}\left(\dfrac{1 \pm A}{1 + A}\right) & \text{for } A \geq 0.5, \\ \left(\dfrac{1 \pm A}{1 + A}\right) & \text{for } A < 0.5, \end{cases}$$

evaluated here for $A = 0.67$, where the subscript b/s represents values for the bubble or spike and the plus sign is used for the bubble growth

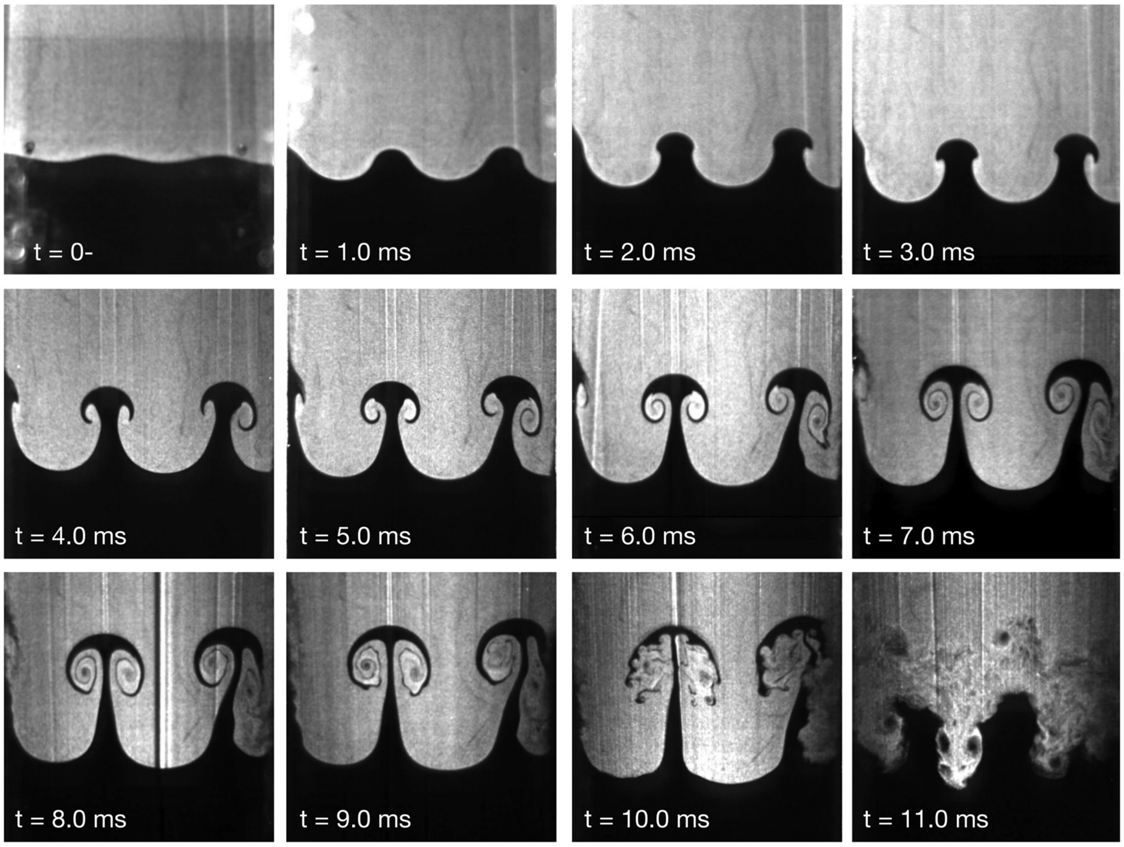

FIG. 5. Image sequence of an air/SF_6 experiment.

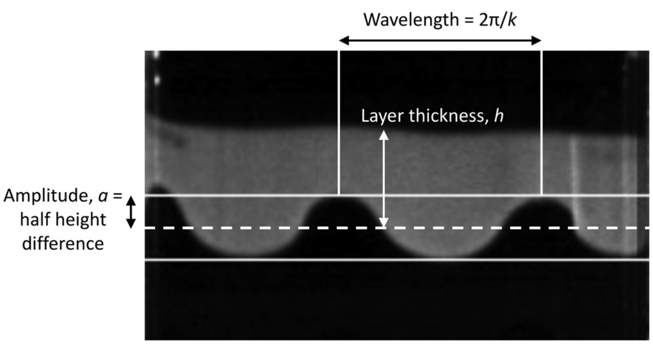

FIG. 6. Illustration showing the definitions of perturbation amplitude, wavelength, and layer thickness.

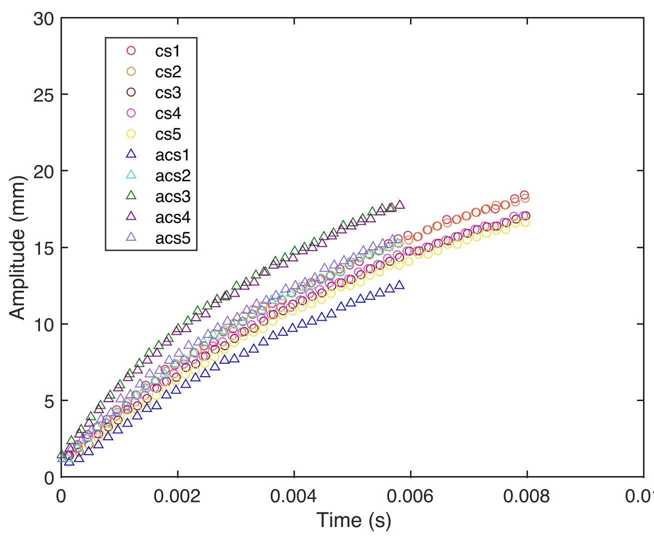

FIG. 7. Dimensional amplitudes of the five air/CO_2/SF_6 experiments as well as the five CO_2/SF_6 experiments over time. Here, the format *cs#* denotes a CO_2/SF_6 experiment and the chronological order in which it was run. Likewise, *acs#* denotes an air/CO_2/SF_6 experiment and the chronological order in which it was run.

rate and the minus sign for the spike. As has been shown for our previous single-interface experiments,[29] the model shows good agreement with the present air/SF_6 amplitude measurements.

To quantify these differences further, Fig. 11 shows the mean values of the amplitudes for the experiments comprising the two groups: air/CO_2/SF_6 and CO_2/SF_6. In each case, the plot symbols indicate mean values, while error bars indicate the 95% confidence intervals

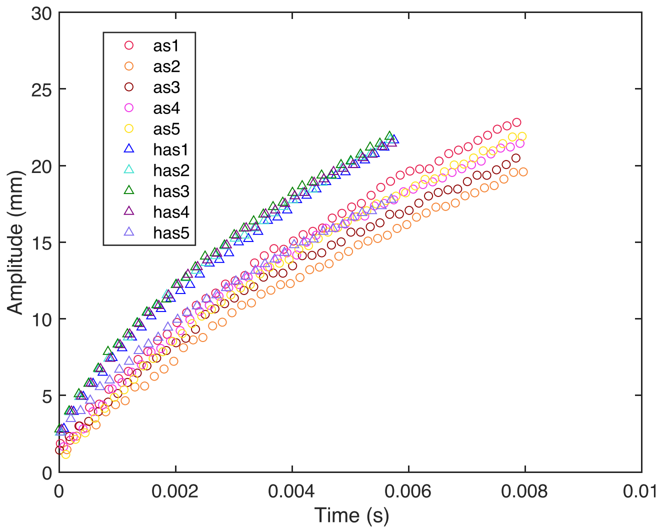

FIG. 8. Dimensional amplitudes of the five He/air/SF_6 experiments as well as the five air/SF_6 experiments over time. The format *as#* denotes an air/SF_6 experiment and the chronological order in which it was run. Likewise, *has#* denotes a He/air/SF_6 experiment and the chronological order in which it was run.

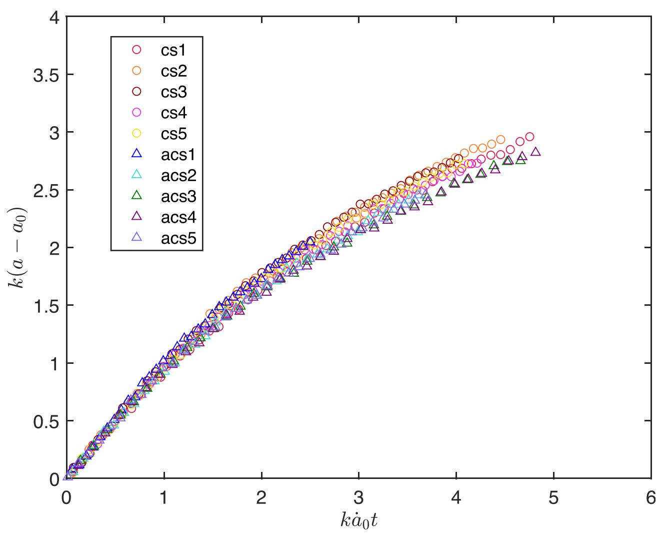

FIG. 9. Data of Fig. 7 in nondimensionalized variables.

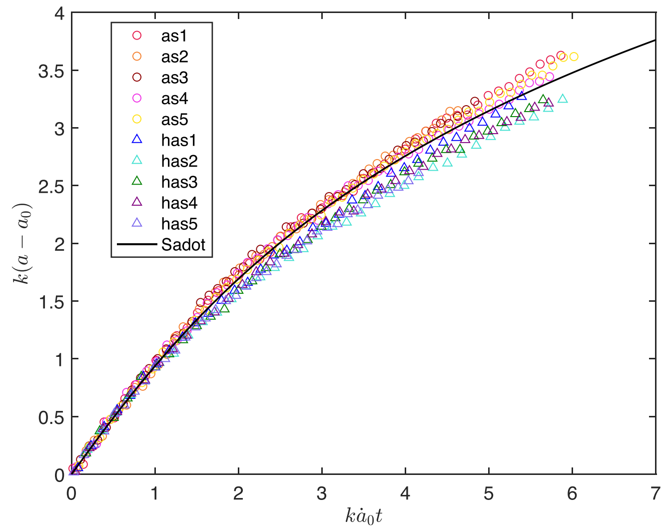

FIG. 10. Data of Fig. 8 in nondimensionalized variables alongside expected behavior as modeled by Sadot *et al.*

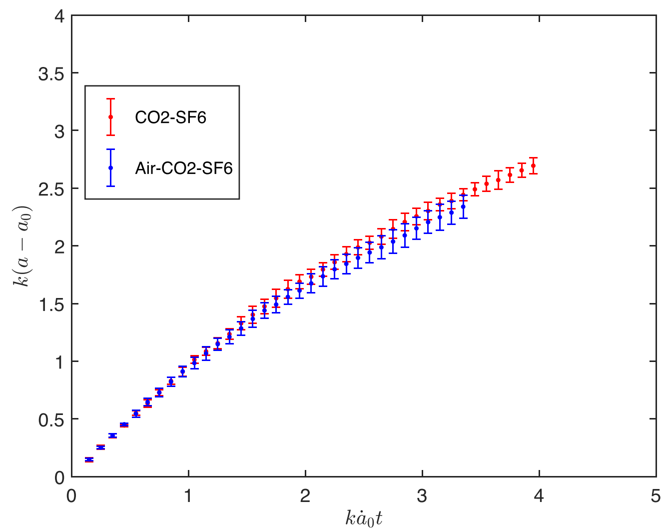

FIG. 11. Mean values for air/CO_2/SF_6 and CO_2/SF_6 with confidence intervals shown as error bars.

calculated from the assumed random variation of the values comprising the means at each time instant. Of note is the fact that the mean values indicate a small difference with the single-interface amplitude lying above that of the two-interface amplitude. However, as is also indicated on this plot, the difference between the air/CO_2/SF_6 and CO_2/SF_6 mean measurements is less than the sum of the confidence intervals, indicating that the observed difference is statistically insufficient to show a measurable difference with 95% confidence.

In contrast, Fig. 12 shows a similar plot this time comparing the air/SF_6 experiments with those of He/air/SF_6. Again, plotted symbols indicate mean values with error bars indicating 95% confidence intervals. However, in this case, the differences lie outside the sum of the confidence intervals for late times when $k\dot{a}_0 t > 2$, showing a statistically significant difference between the two cases. Thus, the presence of the He/air interface above the air/SF_6 interface does indeed appear to produce reduced growth.

The results above indicate that the presence of a second heavy over light gas interface above the primary Richtmyer–Meshkov instability affects the growth at late times by reducing the growth rate. This fact is clearly observed with the larger Atwood number He/air/SF_6 experiments. This difference was also observed with the air/CO_2/SF_6 experiments, but to a lesser degree, with measured difference in mean

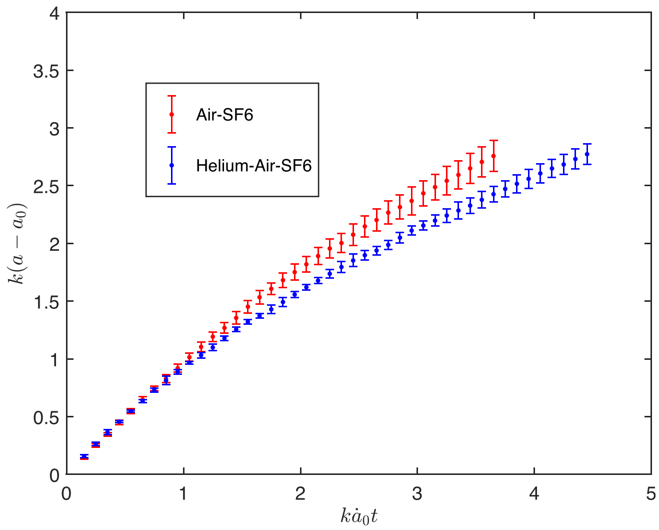

FIG. 12. Mean values for He/air/SF_6 and air/SF_6 with confidence intervals shown as error bars.

values found not sufficient to be statistically significant. Additional experiments increasing the number of measurements used in finding the mean values would be necessary to show this difference for the lower Atwood number experiments.

It should be noted that baroclinic vorticity production does not end after shock passage. Since both interfaces contain substantial density differences, pressure gradients produced by the flow field of the developing instability could result in additional vorticity production. One situation in which this will occur is when the spike tips from the developing RMI on the lower interface approach and come near to the upper unperturbed interface. In this case, the vortical structures present in the spikes would be expected to produce pressure gradients that when combined with the density gradient at the upper interface would result in additional secondary vorticity production. Depending on the distribution of this secondary vorticity, one might expect it to produce a velocity field, resulting in a reduction of spike growth. Since the strength of this secondary vorticity would be larger for a larger density difference, this could explain why the He/air/SF_6 experiments show a greater effect on the developing RMI than do the air/CO_2/SF_6 experiments.

IV. CONCLUSIONS

Shock tube experiments are presented to study the Richtmyer–Meshkov instability of two closely spaced interfaces. Two stably stratified systems of three gases: air, CO_2, and SF_6 and He, air, and SF_6 were formed in a vertical shock tube such that an approximately 30-mm thick layer of intermediate-density gas (either CO_2 or air) is separated from a lighter gas (either air or helium) from above and a heavy gas (SF_6) from below. A two-dimensional sinusoidal perturbation was then generated on the lower interface by horizontally oscillating the shock tube test section. The passage of a weak shock wave generated by bursting the shock tube diaphragm then produces the instability. Amplitude measurements of the perturbation on the lower interface have shapes similar to those of a typical similar single-interface instability. However, when compared with single-interface CO_2/SF_6 or air/SF_6 control experiments, it is found that the presence of the upper unperturbed interface results in reduced growth during the nonlinear growth phase. It is found that the observed reduction in growth is not statistically significant for the lower Atwood number air/CO_2/SF_6 experiments but is statistically significant for the larger Atwood number He/air/SF_6 experiments. One possible cause for the reduction of growth when a second interface lies above the perturbed interface could be the result of secondary baroclinic vorticity produced by the interaction of the density gradient at the upper interface with the pressure field induced by the approaching spike vortical structures.

ACKNOWLEDGMENTS

The software used in this work was developed in part by the DOE NNSA and DOE Office of Science-supported Flash Center for Computational Science at the University of Chicago and the University of Rochester. This work was performed under the auspices of the U.S. Department of Energy by Lawrence Livermore National Laboratory under Contract No. DE-AC52-07NA27344. The work at the University of Arizona was supported by LLNL Subcontract No. B645527 and by the U.S. Department of Energy National Nuclear Security Administration under the Stewardship Science Academic Alliances program through DOE Research Grant No. DE-NA0003903.

AUTHOR DECLARATIONS

Conflict of Interest

The authors have no conflicts to disclose.

Author Contributions

Mark Schalles: Formal analysis (equal); Investigation (equal); Methodology (equal); Software (equal); Visualization (equal); Writing – original draft (equal). **Carlton Martin Louie:** Investigation (equal); Methodology (equal). **Kyle Peabody:** Formal analysis (equal); Investigation (equal); Methodology (equal). **James D. Sadler:** Validation (equal). **Ye Zhou:** Funding acquisition (equal); Project administration (equal); Validation (equal). **Jeffrey W. Jacobs:** Conceptualization (lead); Data curation (equal); Formal analysis (equal); Funding acquisition (equal); Methodology (equal); Project administration (equal); Resources (equal); Supervision (equal); Writing – original draft (equal).

DATA AVAILABILITY

The data that support the findings of this study are available from the corresponding author upon reasonable request.

REFERENCES

[1]R. D. Richtmyer, "Taylor instability in shock acceleration of compressible fluids," Commun. Pure Appl. Math. **13**, 297 (1960).
[2]E. E. Meshkov, "Instability of the interface of two gases accelerated by a shock wave," Fluid Dyn. **4**, 101–104 (1969).
[3]W. D. Arnett, J. N. Bahcall, R. P. Kirshner, and S. E. Woosley, "Supernova 1987A," Annu. Rev. Astron. Astrophys. **27**, 629 (1989).
[4]J. Yang, T. Kubota, and E. E. Zukoski, "Applications of shock-induced mixing to supersonic combustion," AIAA J. **31**(5), 854–862 (1993).
[5]J. D. Lindl, *Inertial Confinement Fusion* (Springer, New York, 1998).

[6] Y. Zhou, "Rayleigh–Taylor and Richtmyer–Meshkov instability induced flow, turbulence, and mixing. I," Phys. Rep. **720–722**, 1–136 (2017).
[7] Y. Zhou, "Rayleigh–Taylor and Richtmyer–Meshkov instability induced flow, turbulence, and mixing. II," Phys. Rep. **723–725**, 1–160 (2017).
[8] Y. Zhou, T. T. Clark, D. S. Clark, S. G. Glendinning, M. A. Skinner, C. M. Huntington, O. A. Hurricane, A. M. Dimits, and B. A. Remington, "Turbulent mixing and transition criteria of flows induced by hydrodynamic instabilities," Phys. Plasmas **26**, 080901 (2019).
[9] Y. Zhou, R. J. Williams, P. Ramaprabhu, M. Groom, B. Thornber, A. Hillier, W. Mostert, B. Rollin, S. Balachandar, P. D. Powell, A. Mahalov, and N. Attal, "Rayleigh–Taylor and Richtmyer–Meshkov instabilities: A journey through scales," Physica D **423**, 132838 (2021).
[10] M. Mohaghar, J. Carter, G. Pathikonda, and D. Ranjan, "The transition to turbulence in shock-driven mixing: Effects of Mach number and initial conditions," J. Fluid Mech. **871**, 595 (2019).
[11] M. Mohaghar, J. McFarland, and D. Ranjan, "Three-dimensional simulations of reshocked inclined Richtmyer-Meshkov instability: Effects of initial perturbations," Phys. Rev. Fluids **7**, 093902 (2022).
[12] P. Suchandra and D. Ranjan, "Dynamics of multilayer Rayleigh–Taylor instability at moderately high Atwood numbers," J. Fluid Mech. **974**, A35 (2023).
[13] C. D. Noble, J. M. Herzog, A. M. Ames, J. Oakley, D. A. Rothamer, and R. Bonazza, "High speed PLIF study of the Richtmyer–Meshkov instability upon re-shock," Physica D **410**, 132519 (2020).
[14] C. D. Noble, J. M. Herzog, D. A. Rothamer, A. M. Ames, J. Oakley, and R. Bonazza, "Scalar power spectra and scalar structure function evolution in the Richtmyer–Meshkov instability upon reshock," J. Fluids Eng. **142**, 121102 (2020).
[15] C. Noble, A. Ames, R. McConnell, J. Oakley, D. Rothamer, and R. Bonazza, "Simultaneous measurements of kinetic and scalar energy spectrum time evolution in the Richtmyer–Meshkov instability upon reshock," J. Fluid Mech. **975**, A39 (2023).
[16] K. O. Mikaelian, "Richtmyer-Meshkov instabilities in stratified fluids," Phys. Rev. A **31**, 410 (1985).
[17] K. O. Mikaelian, "Rayleigh–Taylor and Richtmyer–Meshkov instabilities in finite-thickness fluid layers," Phys. Fluids **7**, 888–890 (1995).
[18] K. O. Mikaelian, "Numerical simulations of Richtmyer–Meshkov instabilities in finite-thickness fluid layers," Phys. Fluids **8**, 1269–1292 (1996).
[19] K. O. Mikaelian, "Rayleigh-Taylor and Richtmyer-Meshkov instabilities and mixing in stratified cylindrical shells," Phys. Fluids **17**, 094105 (2005).
[20] M. Henry de Frahan, P. Movahed, and E. Johnsen, "Numerical simulations of a shock interacting with successive interfaces using the discontinuous Galerkin method: The multilayered Richtmyer–Meshkov and Rayleigh–Taylor instabilities," Shock Waves **25**, 329–345 (2015).
[21] Y. Liang, L. Liu, Z. Zhai, T. Si, and C.-Y. Wen, "Evolution of shock accelerated heavy gas layer," J. Fluid Mech. **886**, A7 (2020).
[22] Y. Liang and X. Luo, "Shock-induced dual-layer evolution," J. Fluid Mech. **929**, R3 (2021).
[23] Y. Liang and X. Luo, "On shock-induced heavy-fluid-layer evolution," J. Fluid Mech. **920**, A13 (2021).
[24] Y. Liang and X. Luo, "On shock-induced light-fluid-layer evolution," J. Fluid Mech. **933**, A10 (2022).
[25] Y. Liang and X. Luo, "On shock-induced evolution of a gas layer with two fast/slow interfaces," J. Fluid Mech. **939**, A16 (2022).
[26] Y. Liang and X. Luo, "Hydrodynamic instabilities of two successive slow/fast interfaces induced by a weak shock," J. Fluid Mech. **955**, A40 (2023).
[27] M. A. Jones and J. W. Jacobs, "A membraneless experiment for the study of Richtmyer-Meshkov instability," Phys. Fluids **9**, 3078 (1997).
[28] B. D. Collins and J. W. Jacobs, "PLIF flow visualization and measurements of the Richtmyer-Meshkov instability of an air/SF_6 interface," J. Fluid Mech. **464**, 113 (2002).
[29] J. W. Jacobs and V. V. Krivets, "Experiments on the late-time development of single-mode Richtmyer-Meshkov instability," Phys. Fluids **17**, 034105 (2005).
[30] R. V. Morgan, R. Aure, J. Stockero, J. Greenough, W. Cabot, O. Likhachev, and J. Jacobs, "On the late time growth of the two-dimensional Richtmyer–Meshkov instability in shock tube experiments," J. Fluid Mech. **712**, 354–383 (2012).
[31] C. C. Long, V. V. Krivets, J. A. Greenough, and J. W. Jacobs, "Shock tube experiments and numerical simulation of the single-mode, three-dimensional Richtmyer-Meshkov instability," Phys. Fluids **21**, 114104 (2009).
[32] J. W. Jacobs, V. V. Krivets, V. Tsiklashvili, and O. A. Likhachev, "Experiments on the Richtmyer-Meshkov instability with an imposed, random initial perturbation," Shock Waves **23**, 407–413 (2013).
[33] E. Sewell, K. Ferguson, V. Krivets, and J. Jacobs, "Time-resolved particle image velocimetry measurements of the turbulent Richtmyer–Meshkov instability," J. Fluid Mech. **917**, A41 (2021).
[34] O. Sadot, L. Erez, U. Alon, D. Oron, L. A. Levin, G. Erez, G. Ben-Dor, and D. Shvarts, "Study of nonlinear evolution of single-mode and two-bubble interaction under Richtmyer-Meshkov instability," Phys. Rev. Lett. **80**, 1654 (1998).